

Preparation and Characterization of Polymer Composite Materials Based on PLA/TiO₂ for Antibacterial Packaging

Edwin A. Segura González ^{1,2}, Dania Olmos ^{2,*}, Miguel Ángel Lorente ², Itziar Vélaz ³ and Javier González-Benito ^{2,*}

¹ Dirección de Investigación, Universidad Interamericana de Panamá, Ciudad de Panamá, Panamá; edwin_segura@uip.edu.pa

² Department of Materials Science and Engineering and Chemical Engineering, Instituto de Química y Materiales Álvaro Alonso Barba (IQMAA), Universidad Carlos III de Madrid, Leganés 28911, Madrid, Spain; malorente@ing.uc3m.es

³ Departamento de Química, Facultad de Ciencias, Universidad de Navarra, 31080 Pamplona, Navarra, Spain; itzvelaz@unav.es

* Correspondence: dolmos@ing.uc3m.es (D.O.); javid@ing.uc3m.es (J.G.-B.); Tel.: +34-916249447 (D.O.); +34-916248870 (J.G.-B.)

Received: date; Accepted: date; Published: date

3. Results and discussion

3.1. Structural characterization.

X-Ray Diffraction

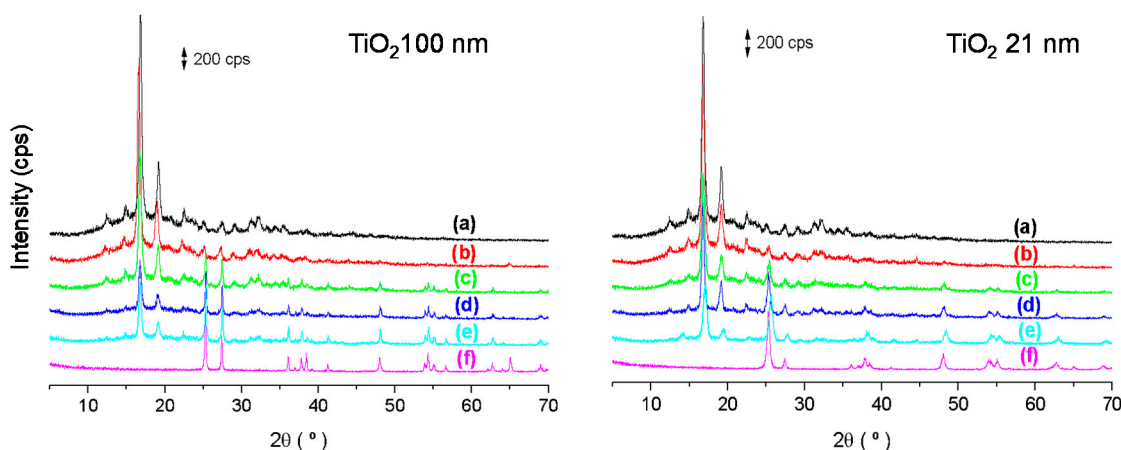


Figure S1.-X-Ray Diffraction patterns for the samples with TiO₂-100nm (left) and TiO₂-21nm (right) as a function of the content in TiO₂ nanoparticles: a) PLA-0; b) PLA/TiO₂-1; c) PLA/TiO₂-5; d) PLA/TiO₂-10; e) PLA/TiO₂-20 and f) pure TiO₂-100nm (left) or pure TiO₂-21 nm (right).

In both plots, the characteristic peaks of PLA-0 and TiO₂ were observed. Crystalline peaks in the nanocomposite materials associated with PLA appear in the interval of 2 θ = 15-25°. As the content of nanoparticles increases in the polymer matrix, the appearance of peaks from TiO₂ can

be observed. The peaks associated to TiO₂ showed lines that belonged to both anatase and rutile (see **Table S1**).

Table S1. XRD peaks of both polymorphs of TiO₂.

TiO ₂ (Rutile)		TiO ₂ (Anatase)	
2θ (°)	(hkl)	2θ (°)	(hkl)
27.4	110	25.3	101
36.1	101	36.9	112
41.2	111	37.8	004
54.3	211	38.4	112
56.6	220	48.0	200
64.0	310	53.9	105
65.0	221	55.0	211
		62.7	215/204
		69	116

Fourier Transformed Infrared Spectroscopy (FTIR)

Table S2. Band assignment for the PLA infrared spectrum in the MID-IR region ^{1,2}

Frequency (cm ⁻¹)	Band assignment	Frequency (cm ⁻¹)	Band assignment
2997	ν _{as} (CH ₃)	1209	ν _{as} (COC) + ρ _{as} (CH ₃)
2945	ν _s (CH ₃)	1180	⊙ _{as} COC + ρ _{as} CH ₃)
2920	⊙ _{as} (CH ₂)	1128	ρ _{as} (CH ₃)
2881	⊙(CH ₃)	1082	⊙ _s (COC)
2850	⊙ _s (CH ₂)	1043	⊙(C-CH ₃)
1747	⊙(C=O)	957	CH ₃ + ⊙CC
1452	δ _{as} (CH ₃)	918	ρ(CH ₃ + ⊙CC)
1381	δ _s (CH ₃)	868	⊙(C-COO)
1359	δ _{as} (CH ₃)	756	δ(C=O)
1304	δ(CH)	700	γ(C=O)
1267	⊙ _{as} (COC) + δ(CH)		

¹Auras R et al. *Macromol Biosci* 2004;4: 835–64. ²Krikorian V, Pochan DJ. *Macromolecules* 2005; 38: 6520–7.

3.2. Thermal characterization.

Differential Scanning Calorimetry (DSC)

Table S3. Characteristic transition temperatures (T_g , T_c and T_m) obtained from the second heating scan in DSC experiments.

Sample	T_g (°C)	T_c (°C)	T_m (°C)
PLA-0	64.6	136.9	166.8
PLA/TiO ₂ -100-1	64.5	137.5	167.4
PLA/TiO ₂ -100-5	64.2	137.2	167.1
PLA/TiO ₂ -100-10	64.5	136.7	166.7
PLA/TiO ₂ -100-20	64.5	136.9	167.7
PLA/TiO ₂ -21-1	64.6	136.9	167.8
PLA/TiO ₂ -21-5	64.6	136.9	166.5
PLA/TiO ₂ -21-10	64.8	137.4	167.9
PLA/TiO ₂ -21-20	65.3	136.3	167.4

Thermogravimetry Analysis (TGA)

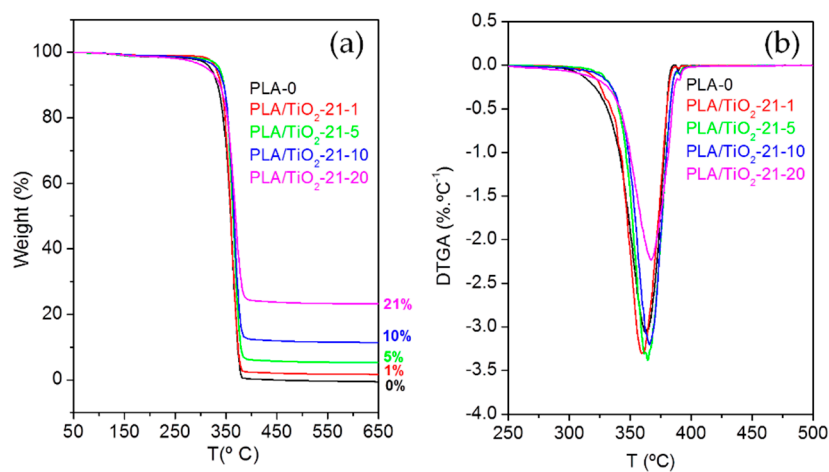


Figure S2. (a) Thermogravimetric analysis curve and (b) DTGA curve for the systems based on PLA/TiO₂-21.

3.3. Antimicrobial behaviour.

3.3.1. Study of biofilm development on the surface of the materials

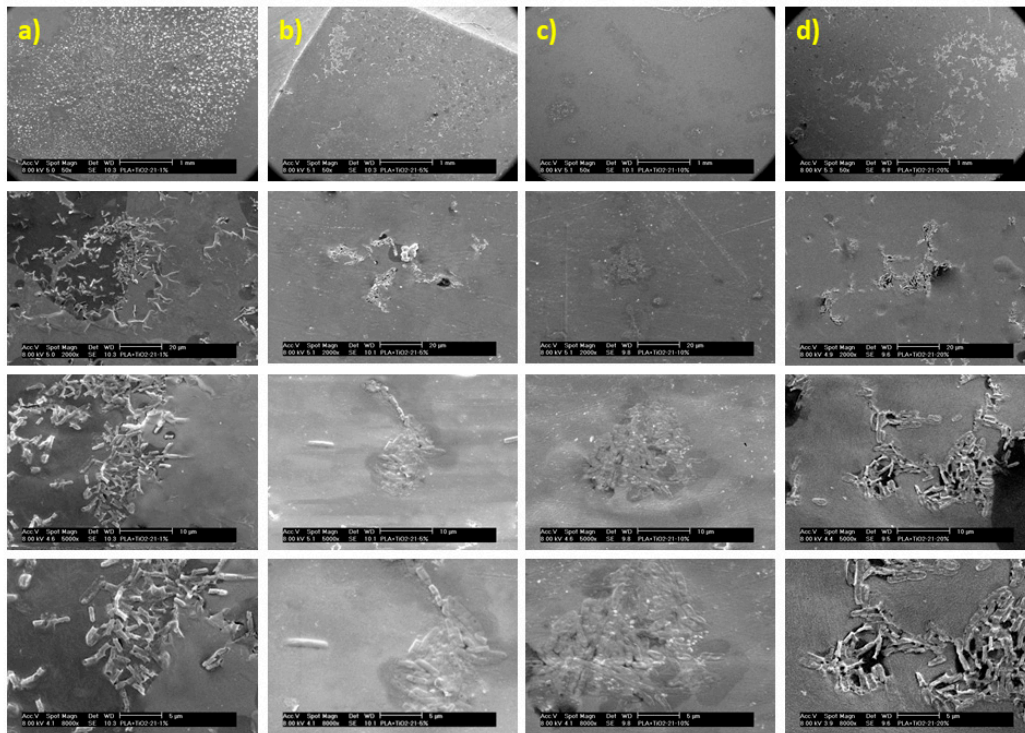


Figure S3. From top to bottom: Each row corresponds to SEM micrographs obtained at different magnifications: 50 ×; 2000 ×; 5000 × and 8000 × PLA/TiO₂ nanocomposite materials ($\phi \sim 21$ nm) as a function of the content in TiO₂ nanoparticles in each column: a) 1%; b) 5%; c) 10% and d) 20% (wt%).

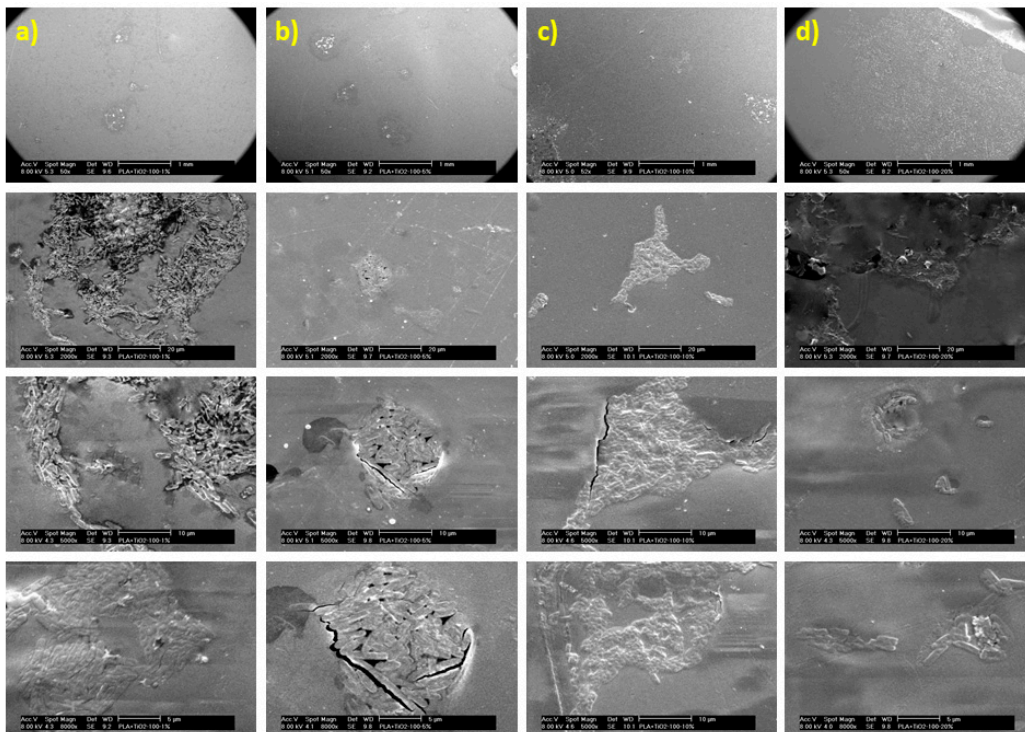


Figure S4. From top to bottom: Each row corresponds to SEM micrographs obtained at different magnifications: 50 ×; 2000 ×; 5000 × and 8000 × PLA/TiO₂ nanocomposite materials ($\phi < 100$ nm) as a function of the content in TiO₂ nanoparticles in each column: a) 1%; b) 5%; c) 10% and d) 20% (wt%).